



Demonstration of quasi-phase-matched nonreciprocal polarization rotation in III-V semiconductor waveguides incorporating magneto-optic upper claddings

B. M. Holmes and D. C. Hutchings

Citation: [Applied Physics Letters](#) **88**, 061116 (2006); doi: 10.1063/1.2172648

View online: <http://dx.doi.org/10.1063/1.2172648>

View Table of Contents: <http://scitation.aip.org/content/aip/journal/apl/88/6?ver=pdfcov>

Published by the [AIP Publishing](#)

Articles you may be interested in

[Near-infrared optical parametric oscillator in a III-V semiconductor waveguide](#)

Appl. Phys. Lett. **103**, 261105 (2013); 10.1063/1.4853595

[Second harmonic generation in phase matched aluminum nitride waveguides and micro-ring resonators](#)

Appl. Phys. Lett. **100**, 223501 (2012); 10.1063/1.4722941

[A compact, broadband slot waveguide polarization rotator](#)

AIP Advances **1**, 042136 (2011); 10.1063/1.3662034

[All-optical diode in a periodically poled lithium niobate waveguide](#)

Appl. Phys. Lett. **79**, 314 (2001); 10.1063/1.1386407

[Patterned birefringence by photoinduced depoling in electro-optic polymers and its application to a waveguide polarization splitter](#)

Appl. Phys. Lett. **73**, 3052 (1998); 10.1063/1.122669

The banner features a blue background with a molecular structure of spheres and rods. On the left is a thumbnail image of an 'AIP Applied Physics Reviews' journal cover, which shows a 3D grid structure. To the right of the thumbnail, the text 'NEW Special Topic Sections' is written in large, white, sans-serif font. Below this, the text 'NOW ONLINE' is in yellow, followed by 'Lithium Niobate Properties and Applications: Reviews of Emerging Trends' in white. The AIP Applied Physics Reviews logo is in the bottom right corner.

NEW Special Topic Sections

NOW ONLINE
Lithium Niobate Properties and Applications:
Reviews of Emerging Trends

AIP Applied Physics Reviews

Demonstration of quasi-phase-matched nonreciprocal polarization rotation in III-V semiconductor waveguides incorporating magneto-optic upper claddings

B. M. Holmes^{a)} and D. C. Hutchings

Department of Electronics and Electrical Engineering, University of Glasgow, Glasgow, United Kingdom

(Received 30 September 2005; accepted 16 January 2006; published online 9 February 2006)

The demonstration of quasi-phase-matched nonreciprocal polarization rotation in a waveguide comprising a conventional III-V semiconductor core and lower cladding is reported. The approach, which is achieved through the incorporation of a periodic upper cladding that alternates between magneto-optic and nonmagneto-optic media, overcomes many of the problems traditionally encountered when transferring the principles of free-space Faraday-effect optical isolators into waveguide geometries. An enhancement of polarization rotation many times greater than that achievable in the absence of phase matching is observed. Additionally, the technique facilitates an ability to select and/or manipulate individual modes from multimode waveguides. © 2006 American Institute of Physics. [DOI: 10.1063/1.2172648]

Current and next-generation wafer scale photonic integrated circuits necessitate stable integrated optical sources free from the “injection noise” that arises as a consequence of emitted radiation being reflected back into the laser cavity.¹ In order to achieve this stability currently, bulk optical-isolators [which conventionally exploit magneto-optic (MO) Faraday rotation] are incorporated between the laser source and the rest of the optical system. Their assembly is a labor intensive process that results in increased cost and reduced throughput. The prospect of monolithically integrated laser/optical isolators has attracted considerable attention and there are several novel approaches. However, there are a number of inherent difficulties when transferring the principles of bulk isolators to waveguides. This letter provides innovative solutions to some of these challenges and provides a demonstration of quasi-phase-matched nonreciprocal polarization rotation in waveguides comprising a III-V semiconductor core and lower cladding.

MO materials with large Verdet constants, which give a measure of a material’s ability to rotate polarization as a function of applied field and transmission length, are generally found to possess relatively low refractive indices compared to those of III-V semiconductors, such as GaAs. Conventional III-V semiconductors, in turn, possess extremely small Verdet constants. In order to effectively guide light, the refractive index of the core layer must normally be greater than that of the cladding layers. This therefore precludes the incorporation of conventional MO materials as waveguide core layers in III-V structures. However, this dichotomy may be circumvented through the integration of the MO media as an upper cladding layer.^{2,3} Consequently, only the evanescent tail of the guided mode interacts with the MO media, enabling the integration of a laser and Faraday effect isolator utilizing a continuous III-V waveguide core. The overlap integral reduces the MO interaction to typically a few percent of that in the MO media alone, but this can be accommodated with a commensurate increase in device length.

A further difficulty arises as a consequence of the inherent structural birefringence associated with waveguide geometries, which leads to a phase mismatch between the shape birefringence ($\Delta\beta_s$) and the much smaller MO birefringence ($\Delta\beta_{MO}$). As a result, the induced polarization rotation has an oscillatory behavior, which limits the degree of rotation obtainable (Fig. 1), with a characteristic beat length of period $2L_{\Delta\beta}$, where

$$L_{\Delta\beta} = \frac{\pi}{\sqrt{(\Delta\beta_s)^2 + (\Delta\beta_{MO})^2}} \approx \frac{\pi}{\Delta\beta_s}. \quad (1)$$

The adoption of a quasi-phase-matching (QPM) approach, which may be implemented through a periodic reversal of the applied magnetic field every beat length, removes this restriction in the obtainable polarization rotation (Fig. 1). QPM by an alternating magnetic field has been demonstrated through the use of a serpentine current loop⁴ and by a periodic localized annealing of the MO media.⁵ However, these designs, based on a MO waveguide core, have to overcome any complications arising from magnetic field edge effects and potential demagnetization at the interfaces between the alternately magnetised elements, which become exacerbated at small beat lengths.

It has been recognized in the field of nonlinear optics that QPM of frequency generation only requires a modulation in the nonlinear coefficient and not necessarily its com-

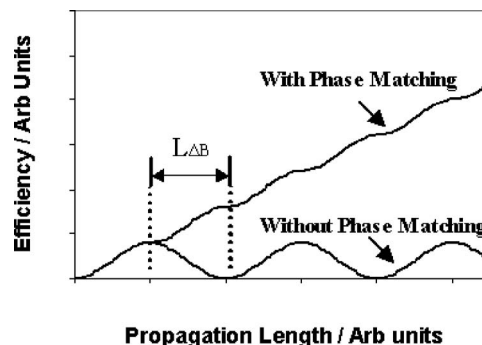


FIG. 1. Schematic demonstrating QPM by periodic domain reversal.

^{a)}Electronic mail: b.holmes@elec.gla.ac.uk

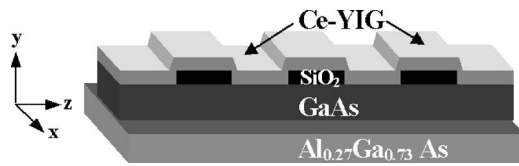


FIG. 2. Schematic of QPM waveguiding structure.

plete reversal (the conversion is determined by the appropriate Fourier coefficient).⁶ This approach is extended here to Faraday rotation by utilizing an upper cladding that periodically alternates between MO and non-MO media. Careful selection of materials of a similar refractive index to the MO upper cladding ensures that the required waveguiding and phase-matching conditions are achieved and scattering losses are minimized. Moreover, this method only requires a mono-directional magnetic field; eliminating edge effects and simplifying the magnetization process. This may be implemented through the addition of a ferromagnetic overlayer and hence the complexity and time to produce and operate such devices is greatly reduced.

Preliminary devices, fabricated in order to demonstrate proof-of-principle and depicted schematically in Fig. 2, consist of a $4.7\ \mu\text{m}$ $\text{Al}_{0.27}\text{Ga}_{0.73}\text{As}$ lower cladding and a $0.5\ \mu\text{m}$ GaAs core layer, grown using metalorganic chemical vapor deposition upon a n -GaAs substrate. A $200\ \text{nm}$ SiO_2 hard mask layer was deposited upon the core, then spincoated with Shipley 1818 photoresist (PR) and the sample baked prior to the photolithographic definition of $2.7\ \mu\text{m}$ wide waveguides. The PR mask was developed and pattern transferred into the SiO_2 layer using a CHF_3 dry-etch process. The remaining PR was removed using an O_2 ashing plasma and the GaAs core, plus $100\ \text{nm}$ of the lower cladding, etched in a SiCl_4 plasma. Upon completion of this stage, a new layer of PR was spun onto the sample and exposed through a periodic mask consisting of periods between 100 and $140\ \mu\text{m}$, in steps of $10\ \mu\text{m}$, with a duty cycle of 50% . On developing, a $1:5$ water: hydrofluoric acid solution was used to remove the exposed SiO_2 areas before the remaining PR was removed with a second O_2 ashing plasma. The sample, with a substrate temperature of 60°C , was then sputter coated using a CeYFeO target (achieving $\text{Ce}_1\text{Y}_2\text{Fe}_5\text{O}_x$ stoichiometry measured through the use of energy dispersive x-ray techniques). The ferromagnetic properties of this MO layer were obtained using the longitudinal Kerr effect, yielding a coercivity of $40\ \text{Oe}$ and a squareness of 0.7 . The waveguide geometries and etch depths were confirmed by a scanning electron microscope (SEM) and Dectak profilometer, respectively.

The periodicity of the alternating MO/non-MO upper cladding layer can be clearly observed in the SEM of a completed sample displayed in Fig. 3. The raised sections (magnified image right) incorporate a $200\ \text{nm}$ thick SiO_2 “exclusion” layer between the GaAs core and the CeYFeO upper cladding, effectively eliminating any interaction between the evanescent tail of the guided mode and the MO layer. In contrast, the nonraised sections consist of CeYFeO deposited directly upon the waveguide core, facilitating interaction with the guided modes.

The samples were saturated in a $240\ \text{kA/m}$ ($\sim 3\ \text{kOe}$) magnetic field, applied parallel to the waveguides. The $8\ \text{mm}$ long waveguides were then characterized without an external applied magnetic field, over a wavelength range of

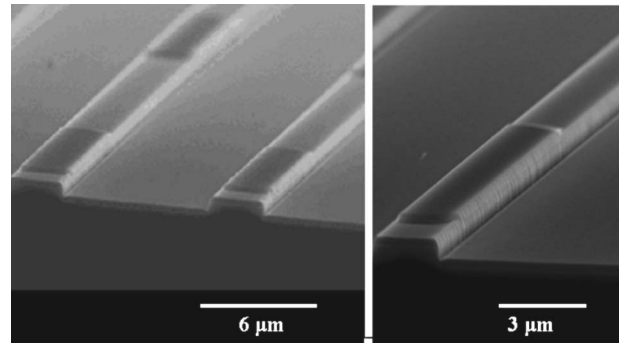


FIG. 3. SEM of the fabricated QPM strip-loaded waveguides.

$1267\text{--}1367\ \text{nm}$, using an Agilent tunable laser. Transverse electric (TE) polarized radiation was coupled into the guides using the end-fire technique and the output passed through a polarising beam-splitting cube in order to separate the TE and transverse magnetic (TM) components. These were then individually detected to obtain the mode conversion efficiencies E_f , where

$$E_f = \frac{P_{\text{TM}}}{P_{\text{TM}} + P_{\text{TE}}} \times 100\% . \quad (2)$$

P_{TM} and P_{TE} are the TM and TE output powers, respectively. Optical losses were estimated using the Fabry–Perot method. Theoretical design and simulation of these types of structures were conducted using a full vectorial mode finder and three-dimensional beam propagation software package.

The TE to TM conversion efficiencies as a function of wavelength are displayed in Fig. 4 for three different periods. Phase matching of the polarization conversion (nominally a

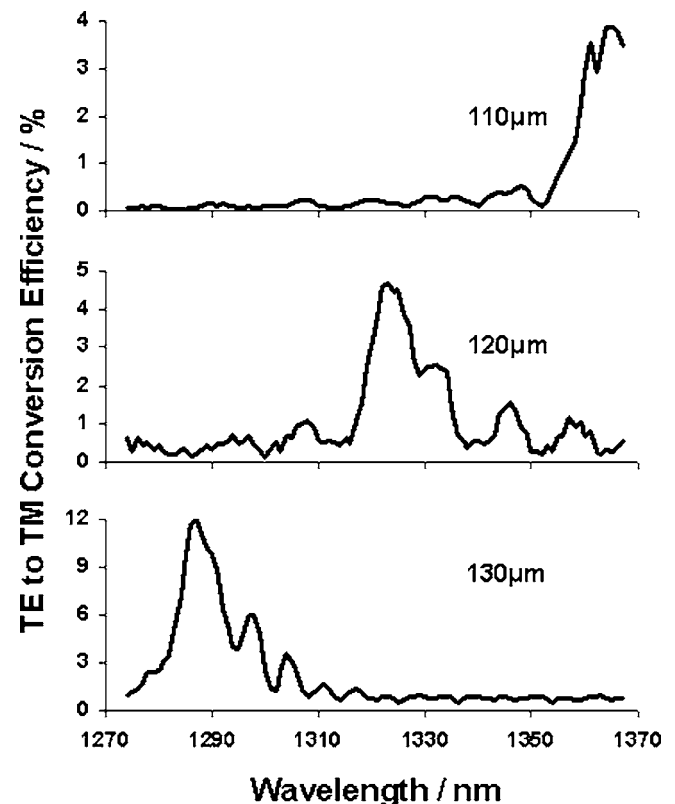


FIG. 4. Polarization conversion efficiency as a function of wavelength for the three different QPM periods indicated.

sinc^2 function) is clearly observed to occur at wavelengths of 1287 nm, 1323 nm, and 1367 nm for periodicities of 130 μm , 120 μm , and 110 μm , respectively. The increase in the mode conversion efficiency of the guides at shorter wavelengths, observed as the period is increased, is primarily attributable to the enhancement of the Verdet coefficient as the wavelength is reduced over the measured range. Commensurately, losses are also observed to increase over this wavelength range, from (0.9 ± 0.1) dB/mm at 1367 nm to (1.2 ± 0.1) dB/mm at 1287 nm.

At present, the largest observed TE to TM mode efficiency is 12%, obtained at a wavelength of 1287 nm. However, the current devices support both the fundamental and first-order modes over the considered wavelength range, and the TE to TM power conversion is found to occur between the TE_2 to TM_1 modes. The measured efficiency includes the output power P_{TE} of both the TE_1 (unconverted) and TE_2 modes. Consequently, it may be assumed that the actual conversion efficiency between the TE_2 and TM_1 modes is substantially larger. Unfortunately, due to the difficulties in determining an accurate value for the relative power levels launched in the TE_1 and TE_2 modes, it has not been possible to obtain a quantitative value for this actual conversion efficiency. Nevertheless, this value still represents an enhancement of Faraday rotation by approximately 60 times that achievable in the absence of phase-matching (measured on waveguides with a continuous MO upper cladding), which corresponds to the 60 periods fabricated within this guide.

The nonreciprocal nature of the devices was confirmed by using a polarizing beamsplitter on a rotation stage to determine the minor axis of the output polarization. At a wavelength of 1287 nm, a minima was found at $+(7.5 \pm 0.5)^\circ$ from the TM normal. A reversal in the direction of the applied saturation field resulted in the minima being located at $-(7.5 \pm 0.5)^\circ$ from the TM normal, i.e., the sense of the Faraday rotation is reversed. Similar behavior is demonstrated by turning the sample around and keeping the remanent magnetization unchanged.

The TE_2 to TM_1 beat lengths, experimentally obtained from the peak QPM conversion, are found to fall within the range predicted from simulations of 2.7 μm wide waveguides with upper claddings consisting of either solely SiO_2 or CeYFeO . The measured beat lengths correspond to an effective refractive index for the MO/non-MO upper cladding of 1.88.

While the mode conversions measured in the present study occur between the TE_2 and TM_1 modes, simulations indicate that conversion between TE_1 and TM_1 , TE_2 and TM_1 , or TE_2 and TM_2 guided modes are all attainable through a simple modification of the periodicity in the MO/non-MO cladding layer. Intriguingly, this ability offers the potential to selectively separate and/or manipulate individual modes of multimode waveguides. For implementation as part of an integrated isolator, the waveguide width should be decreased to ensure single-mode operation and the appropriate period for TE_1/TM_1 interaction employed.

The CeYFeO MO upper cladding used throughout the present study was deposited directly upon the GaAs surface at 60 $^\circ\text{C}$, and was, therefore, almost certainly neither epitaxial nor in its fully crystalline form (cerium-substituted yttrium-iron-garnet, Ce-YIG). Consequently, the Verdet

constant of the media produced, which from the presence of ferromagnetism is considered to consist of Ce-YIG crystallites in an amorphous CeYFeO matrix, was expected to be considerably subdued compared to those commonly measured in Ce-YIG (generally in the order of $3000^\circ/\text{cm}$). At the elevated temperatures normally required for the deposition, or postdeposition rapid annealing of epitaxial Ce-YIG ($\sim 750^\circ\text{C}$),⁷ unprotected GaAs is known to undergo damaging structural changes. Arsenic migration leads to “intermixing” of buried quantum wells,⁸ while Langmuir evaporation results in a roughening of the GaAs surface.⁹ Although it is therefore not possible to anneal the samples prepared in the present investigation without damage, epitaxial MgO buffer layers, as thin as 4.5 nm, grown upon the surface of GaAs have been demonstrated to adequately protect GaAs and preserve the integrity of a quantum well at temperatures in excess of 800 $^\circ\text{C}$.^{10,11} It has further been demonstrated that high-quality YIG (Ref. 12) and Ce-YIG (Ref. 13) may be grown upon MgO and hence it is anticipated that the use of a buffer layer may provide a route to approaching crystalline Verdet constant values.

The difference in refractive indices between SiO_2 ($n \sim 1.5$) and Ce-YIG will lead to a degree of scattering, although it is highly unlikely that this would coincide with a narrowband coherent Bragg scattering condition. Nevertheless, scattering can be reduced by using instead a suitable dielectric of refractive index that more closely matches that of Ce-YIG. Potential candidates that can be deposited as high-quality films on a semiconductor surface are Ta_2O_5 ($n \sim 2.2$) and Si_3N_4 ($n \sim 1.9$).

QPM nonreciprocal Faraday polarization rotation in a III-V waveguiding device has been demonstrated. It is believed that the culmination of these experiments in conjunction with our recently reported reciprocal mode converters¹⁴ will enable the realization of a monolithically integrated laser and Faraday effect isolator, utilizing a continuous III-V waveguiding core layer.

This work was supported by the Engineering and Physical Sciences Research Council.

¹K. E. Stubkjaer and M. B. Small, *IEEE J. Quantum Electron.* **20**, 472 (1984).

²D. C. Hutchings, *J. Appl. Phys. D.* **36**, 2222 (2003).

³H. Yokoi, T. Mizumoto, and H. Iwasaki, *Electron. Lett.* **38**, 1670 (2002).

⁴P. K. Tien, R. J. Martin, R. Wolfe, R. C. Le Craw, and S. L. Blank, *Appl. Phys. Lett.* **21**, 394 (1972).

⁵R. Wolfe, J. Hegarty, J. F. Dillon, Jr., L. C. Luther, G. K. Celler, and L. E. Trimble, *IEEE Trans. Magn.* **21**, 1647 (1985).

⁶D. C. Hutchings and T. C. Kleckner, *J. Opt. Soc. Am. B* **19**, 890 (2002).

⁷S.-Y. Sung, X. Qi, S. K. Mondal, and B. J. H. Stadler, *Mater. Res. Soc. Symp. Proc.* **817**, L8.3.1, (2004).

⁸J. H. Marsh, *Semicond. Sci. Technol.* **8**, 1136 (1993).

⁹E. J. Tarsa, M. De Graef, D. R. Clarke, A. C. Gossard, and J. S. Speck, *J. Appl. Phys.* **73**, 3267 (1993).

¹⁰B. Stadler and A. Gopinath, *IEEE Trans. Magn.* **36**, 3957 (2000).

¹¹M. Z. Tseng, S. Y. Hu, Y. L. Chang, W. N. Jiang, and E. L. Hu, *Appl. Phys. Lett.* **63**, 987 (1993).

¹²R. Karim, S. A. Oliver, and C. Vittona, *IEEE Trans. Magn.* **31**, 3485 (1995).

¹³B. Stadler, K. Vaccaro, P. Yip, J. Lorenzo, Y. Li, and M. Cherif, *IEEE Trans. Magn.* **38**, 1564 (2002).

¹⁴B. M. Holmes and D. C. Hutchings, *IEEE Photonics Technol. Lett.* **18**, 43 (2006).